# Long-term impact risk for (101955) 1999 $RQ_{36}$

Andrea Milani[1], Steven R. Chesley[2], Maria Eugenia Sansaturio[3], Fabrizio Bernardi[4,1], Giovanni B. Valsecchi[4], Oscar Arratia[3]

[1]Department of Mathematics, University of Pisa
Largo Pontecorvo 5, 56127 Pisa, Italy
e-mail: milani@dm.unipi.it
[2]Jet Propulsion Laboratory, Calif. Inst. of Tech.
Pasadena, CA 91109
[3]E.T.S. de Ingenieros Industriales, University of Valladolid
Paseo del Cauce s/n, 47011 Valladolid, Spain
[4]IASF-Roma, INAF
via Fosso del Cavaliere 100, 00133 Roma, Italy

April 29, 2009

**Abstract**

The potentially hazardous asteroid (101955) 1999 $RQ_{36}$ has a possibility of colliding with the Earth in the latter half of the 22nd century, well beyond the traditional 100-year time horizon for routine impact monitoring. The probabilities accumulate to a total impact probability of approximately $10^{-3}$, with a pair of closely related routes to impact in 2182 comprising more than half of the total. The analysis of impact possibilities so far in the future is strongly dependent on the action of the Yarkovsky effect, which raises new challenges in the careful assessment of longer term impact hazards.

Even for asteroids with very precisely determined orbits, a future close approach to Earth can scatter the possible trajectories to the point that the problem becomes like that of a newly discovered asteroid with a weakly determined orbit. If the scattering takes place late

enough so that the target plane uncertainty is dominated by Yarkovsky accelerations then the thermal properties of the asteroid, which are typically unknown, play a major role in the impact assessment. In contrast, if the strong planetary interaction takes place sooner, while the Yarkovsky dispersion is still relatively small compared to that derived from the measurements, then precise modeling of the nongravitational acceleration may be unnecessary.

**Keywords**: Asteroids, Asteroid dynamics, Impact processes, Orbit determination.

**Acronyms:**
IP: Impact Probability [Milani et al. 2005b]
LOV: Line Of Variations [Milani et al. 2005a]
MC: Monte Carlo [Chodas and Yeomans 1999]
TP: Target Plane [Valsecchi et al. 2003]
VA: Virtual Asteroid [Milani et al. 2000a]
VI: Virtual Impactor [Milani et al. 2000a]

# 1 Impact Monitoring over centuries

As the completion of the *Spaceguard Survey* [Morrison 1992] approaches, we need to start thinking how the task of Impact Monitoring [Milani et al. 2005b] will change in the near future and how we will face the next challenges. When almost all the Near Earth Asteroids (NEAs) of a given size range have been discovered and found not to be hazardous in the next 80–100 years, the problem of what could happen over longer time scales remains. Thus the need arises for extending the Impact Monitoring work deeper into the future. This also implies greater consideration of the sources of orbit propagation uncertainty, for instance asteroid-asteroid perturbations or nongravitational perturbations. For both of these, there are model parameters that have to be solved in addition to the initial conditions and that contribute to the prediction uncertainty.

For a well-observed asteroid, taking into account the Yarkovsky effect and propagating for a long time span, the situation becomes in some sense similar to that of a newly discovered asteroid, for which the effects of chaotic motion and the resulting predictability horizon increase the difficulty of detecting possible impacts.

When a NEA has a very well determined orbit, follow-up astrometric observations may not be necessary *now*: if the current ephemeris error is smaller than the observational errors, the orbit is not significantly improved. If the main sources of prediction uncertainty, over the time span to the possible impact, are the nongravitational effects, then physical observations and theoretical modeling are the most important contribution to solve the problem.

An example of the situation above has already occurred with the identification of a very long term possibility of impact for the asteroid (29075) 1950DA [Giorgini et al. 2002]. It has been observed optically for more than 50 years and with radar in 2001; its semimajor axis has a formal uncertainty (post-fit RMS) of $\simeq 100$ m, the ephemeris uncertainty is $< 0''.05$, thus it is currently impossible to improve the orbit by optical astrometry. For the possible impact in 2880 the main source of uncertainty is the dynamical model, especially the Yarkovsky effect.

This paper is organized as follows: in Section 2 we present the case of asteroid (101955) 1999 $RQ_{36}$ and explain why it is especially interesting for long term impact monitoring. In Section 3 we discuss a model for the Yarkovsky effect on this asteroid and its uncertainties. Section 4 presents our Monte Carlo test to detect possible impacts taking into account the main non-gravitational effects. In Section 5 we compare with the results which can be obtained with the current operational impact monitoring methods, in particular explaining why impacts in the year 2182 have a comparatively high probability. Section 6 provides an interpretation of the dynamical behaviour of (101955) as a sequence of phases dominated by different sources of orbit uncertainty. Section 7 discusses the possibility and difficulty of improving the orbit determination at the next apparitions, thus significantly changing the estimates on impact probability. Section 8 discusses how difficult is to deflect this asteroid, in case the possibility of impact was confirmed by later observations, and which is the most appropriate time to do this. The last Section draws our conclusions, including the one that the case of (101955) is not exceptional, in that it is already possible to find another example for which possible collisions in the 22nd century can be obtained.

## 2 Asteroid (101955) 1999 $RQ_{36}$

We need to select a good example as a test case to develop the analytical tools and the know-how for very long term Impact Monitoring.

The Apollo asteroid (101955) 1999 $RQ_{36}$, having been observed astrometrically over almost 7 years and with radar at two separate apparitions, has the lowest formal uncertainty in semimajor axis of any asteroid[1]: 5 m. However, this uncertainty is indeed formal, in that it ignores the dynamical model uncertainty. As we will show later, a reasonable estimate of the Yarkovsky effect on the semimajor axis of 1999 $RQ_{36}$ is around 200 m/yr. Including a Yarkovsky effect model in the orbit determination can change the nominal solution for the initial conditions by an amount more than an order of magnitude larger than the formal uncertainty.

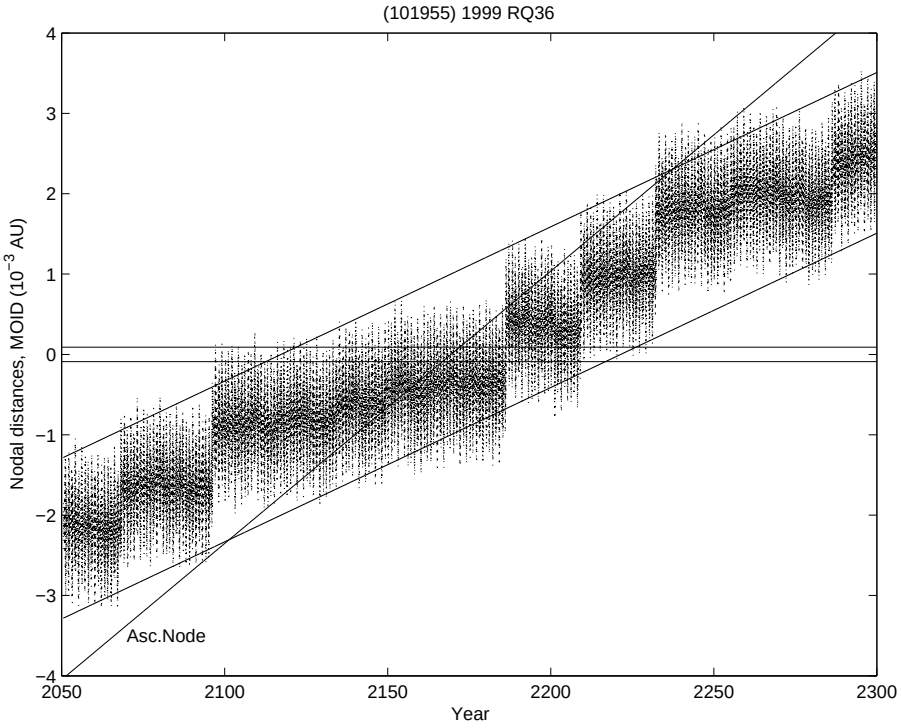


Figure 1: The time evolution of the MOID for (101955) 1999 $RQ_{36}$. The MOID is often less than the effective radius of the Earth (horizontal lines), starting a little before 2100 and until about 2230.

The reason why this asteroid is relevant for long term Impact Monitoring

[1]This minimum uncertainty refers to the initial conditions at the epoch corresponding to the average of the observation times, that is 8 June 2001. For these data, see the NEODyS online system `http://newton.dm.unipi.it/neodys`

is that its Minimum Orbit Intersection Distance (MOID) [Gronchi 2005] is currently low (about one lunar distance) and decreases to near zero at the end of next century. This is shown in Fig. 1, where—to stress the secular evolution—the MOID is represented with sign according to whether the asteroid is outside (positive) or inside (negative) the Earth's orbit at the node crossing. This convention on the sign is as in [Valsecchi et al. 2003], and is the opposite with respect to [Gronchi and Tommei 2006]. The Figure also includes a line (marked "Asc.Node") representing the secular evolution of the nodal distance and two parallel lines representing the secular evolution of the signed MOID.

Thus the secular evolution leads the MOID to cross zero around 2170, with the short periodic perturbations allowing a MOID less than the Earth impact parameter (equal in this case to 2.12 physical Earth radii) at various epochs between 2097 and 2229. This analysis applies to the purely gravitational, nominal solution, for other possible orbits (compatible with the observations) the MOID evolution is similar, that is a node crossing occurs around the same time, although the epochs at which the collisions are possible are different. The node crossing and the growth with time of the along-track position uncertainty are the parameters used in the criteria used to prioritize the Impact Monitoring computations [Milani et al. 2005b, Sec. 2.2]. In other words this asteroid, with currently a very well known orbit, becomes in the 22nd and early 23rd century like a newly discovered *Potentially Hazardous Asteroid* (PHA), with a strongly chaotic orbit.

Considering the discussion above, we have run an Impact Monitoring computation for (101955) 1999 $RQ_{36}$ in the conventional way (with only gravitational effects in the dynamical model) but for a time span longer than usual, until the year 2240. The results were that there are Virtual Impactors (VIs), that is, sets of initial conditions compatible with the observational constraints leading to impacts, in the 2180-2200 time span and with a total Impact Probability (IP) $\simeq 3 \times 10^{-4}$.

However, for the reasons discussed in the previous section, this is not an appropriate way to assess the possibility of an impact and is even poorer for computing the IP. We need to take into account the probabilistic distribution of the parameters appearing in a Yarkovsky model.

# 3 Yarkovsky effect model for 1999 $RQ_{36}$

The main nongravitational perturbation over a time span of centuries is due to the Yarkovsky effect, which is by definition a secular effect and results from the way the asteroid rotation affects the surface temperature distribution and therefore the anisotropic thermal re-emission [Vokrouhlický et al. 2000]. The primary manifestation of the Yarkovsky effect is through a steady drift in semimajor axis:

$$\frac{da}{dt} \propto \frac{\cos\gamma}{\rho R},$$

where $\rho$ is the asteroid's bulk density, $R$ is the asteroid effective radius and $\gamma$ is the angle between the orbital and rotational angular momentum vectors, i.e., the obliquity of the asteroid's equatorial plane with respect to its orbital plane. There is also a complex dependency on the spin rate and surface thermal conductivity $K$, but the main parameter upon which a Yarkovsky model depends is $\cos\gamma$. Thus the sign of the drift in semimajor axis changes when the sense of rotation changes, and the problem is that optical ground-based observations only weakly discriminate the sense of rotation.

Asteroid (101955) 1999 $RQ_{36}$ has been carefully observed during the 2005 encounter with Earth, with optical photometry, radar range and range rate observations. Table 1 lists the assumed model parameters affecting the Yarkovsky effect. The rotation period has been well determined through light-curve analysis (Carl Hergenrother, private communication). For the pole orientation, the analysis of the radar echoes leads to the retrograde solution listed in Table 1 ([Nolan et al. 2007], Nolan, private communication) and the mean radius has also been estimated at 280 m.

From this model it is possible to deduce an a priori estimate of the secular change in semimajor axis $da/dt$, taking Nolan's spin state as accurate enough to contribute little to the uncertainty. With that, the main uncertainties come from density $\rho$, radius $R$ , and thermal conductivity $K$.

First, $da/dt$ varies inversely with $\rho R$. Taking the formal uncertainty in $\rho$ to be 30% and in $R$ to be 15% (these are merely educated guesses) we find that this leads to a 34% uncertainty on $da/dt$. A 20% uncertainty in $da/dt$ due to variations in $K$ can be assumed, because $da/dt$ is only weakly sensitive to $K$; this gives 40% uncertainty on $da/dt$, altogether. The obliquity of 170° obtained from Nolan's pole has some uncertainty, but because the relevant parameter is the cosine of the obliquity this has a modest effect on the uncertainty of the diurnal Yarkovsky contribution. With a nominal $K =$

Table 1: Pole solution and other parameters relevant for the Yarkovsky effect, as assumed in our model for 1999 $RQ_{36}$.

| Parameter | Value | Units |
|---|---|---|
| Pole RA | 102.37 | deg |
| Pole DEC | −52.85 | deg |
| Obliquity $\gamma$ | 169.9 | deg |
| Radius $R$ | 280 | m |
| Albedo | 0.05 | |
| Rotation period | 4.2903 | h |
| Bulk density $\rho$ | $1,500$ | kg/m$^3$ |
| Surface layer density | $1,200$ | kg/m$^3$ |
| Thermal conductivity $K$ | 0.01 | W/m/K |

$10^{-2}$ W/m/K, and following the techniques of [Vokrouhlický et al. 2000], we obtain

$$\frac{da}{dt} = -12.5 \pm 5 \times 10^{-4} \text{ AU/Myr} \ . \tag{1}$$

As an alternative, a plausible range of values for $da/dt$ could be estimated by least squares fit to the astrometric data, including both optical and radar observations. Figure 2 shows a simple method to perform such an estimate, by using 5 separate orbit determinations[2], each one with a different (but constant) value of $da/dt$. The signal is contained in the different values of the fit RMS, which has the value 0.524 assuming no Yarkovsky effect and 0.520 at the minimum. The best fit value is

$$\frac{da}{dt} = -15.0 \pm 9.5 \times 10^{-4} \text{ AU/Myr} \, ,$$

which means that for now we have only a weak detection of the Yarkovsky effect. A similar result has been reported by [Chesley 2008]: the two results are actually identical if the different covariance normalization is taken into account. In the computation of Fig. 2 a simple error model, with optical observations weighted at 1 arcsec, was used. In conclusion the a priori estimate is superior to the ones based on the orbital fit, thus we adopt Eq. (1) as a plausible range.

[2]This fit has used the free software OrbFit, version 3.5.2. OrbFit is available at `http://adams.dm.unipi.it/orbfit/`

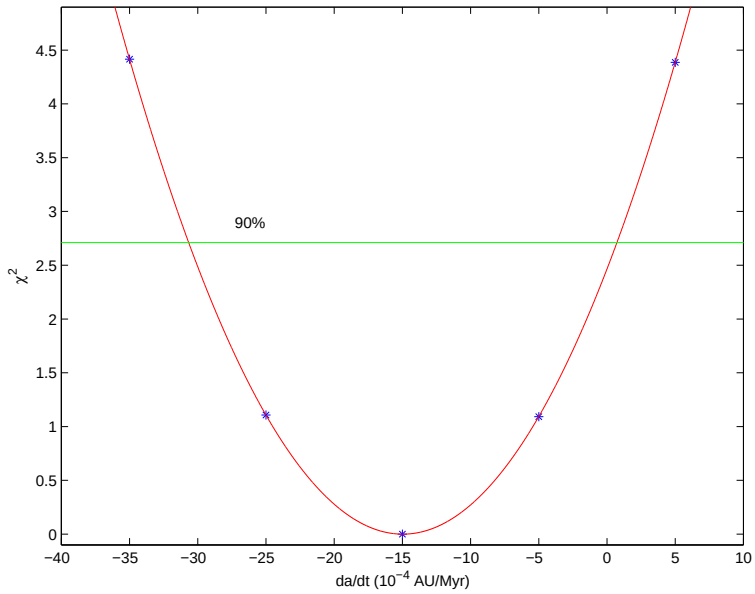


Figure 2: The $\chi^2$ of the least squares fit to the value of $da/dt$. The quadratic approximation for the $\chi^2$ is obtained by a parabola fit to only 5 data points (stars). The horizontal line corresponds to a 90% confidence level for this fit.

# 4 Monte Carlo tests

To assess the possibility of impacts taking into account the Yarkovsky effect with its full uncertainty, we have performed *Monte Carlo* (MC) simulations with the method described in [Chodas and Yeomans 1999]. The MC samples are drawn from a 7-dimensional space of initial conditions, including 6 orbital elements and $da/dt$, based on a normal distribution derived from the a posteriori fit covariance, as obtained from the available observational data and the a priori constraint given by Eq. (1).

Each different MC sample follows its own dynamical route, although the individual sample orbits remain close together for a long time; only after the encounters with the Earth in 2060 and 2080 do they become widely scattered. In Fig. 3 the orbits are plotted shortly after the 2080 encounter, by which time the values for the semimajor axis have been scattered over a range of 0.005 AU.

Out of a sample of $500,000$ initial conditions, which were propagated up to the year 2200, we have found 461 cases of impact. This implies that the

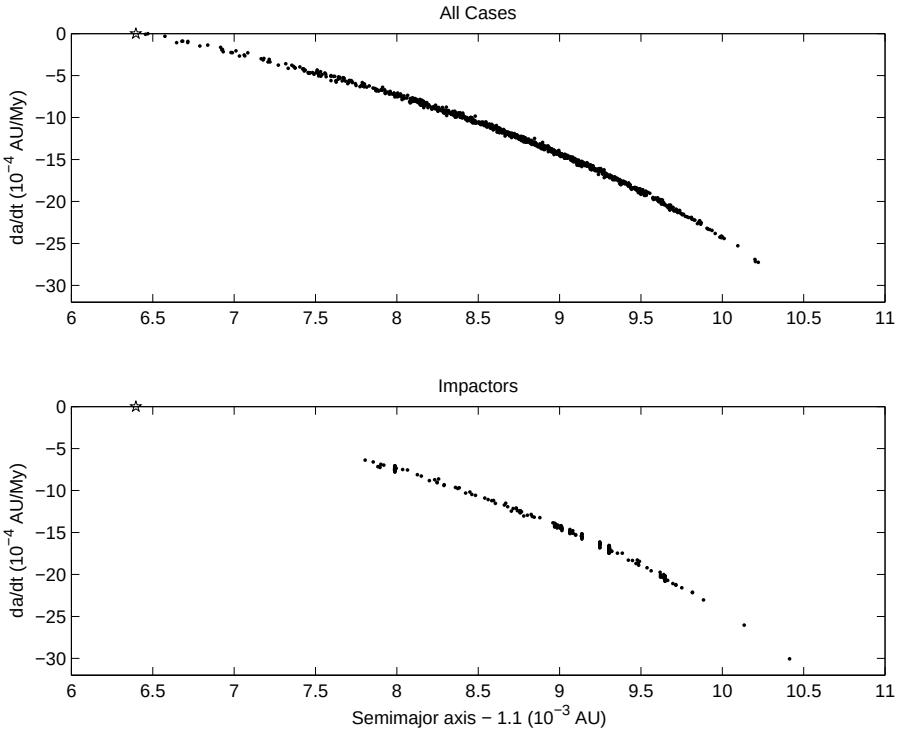


Figure 3: Above: a swarm of Virtual Asteroids (VA), among the 500,000 used in our main Monte Carlo test, plotted in the plane $da/dt$ vs. $a - 1.1$ AU at epoch January 1, 2081. Below: the orbits leading to an impact. The star represents the purely gravitational solution.

overall IP is $\simeq 9.2 \times 10^{-4}$, more than what was obtained by neglecting the Yarkovsky effect altogether. Figure 4 shows the distribution as a function of the Yarkovsky $da/dt$ and of the year of impact. Figure 4 depicts the location and impact probability of the various distinct dynamical routes to impact that are revealed by the Monte Carlo analysis.

Looking for the most significant VIs, we have found that 272 of the 461 impacting Virtual Asteroids (VA) have an impact in the year 2182. Of these, 268 have similar dynamical histories: they appear in Fig. 3 as a narrow strip with $1.1093021 < a < 1.1093076$ AU. Thus there is a single dynamical route leading to an impact in 2182 with an Impact Probability estimated, by the Monte Carlo method, at $\simeq 5.4 \times 10^{-4}$.

Table 2 contains additional details for the cases of the VIs with highest

impact probabilities. Note that the values listed in the Table have not been computed with an automatic, well-documented algorithm, but by ad hoc manipulations. For example, the values of the IP are obtained from the number of impacting VA in the MC run divided by the total number in the sample, the value of the stretching has been deduced from the IP by a simple 1-dimensional formula, similar to the ones of [Milani et al. 2000b, Section 4.3]:

$$S = \frac{C \times \exp(-\sigma_{LOV}^2/2)}{IP \times \sqrt{2\,\pi}} \ ,$$

where $C$ is the chord length corresponding to the crossing of a sphere of radius 2.12 $R_\oplus$ at a distance from the center equal to the minimum occurring for each VI. The value of $\sigma_{LOV}$ has been computed on the basis of the value of $da/dt$.

Table 2: Most Significant VIs for (101955) 1999 $RQ_{36}$ through Year 2200

| $da/dt$ ($10^{-4}$ AU/Myr) | Year | $\sigma_{LOV}$ | Stretch ($R_\oplus$) | IP | Palermo Scale |
|---|---|---|---|---|---|
| −14.60 | 2169/9/24.72 | −0.42 | $9.63 \times 10^4$ | $1.60 \times 10^{-5}$ | −2.73 |
| −17.10 | 2182/9/24.93 | −0.92 | $3.91 \times 10^3$ | $2.60 \times 10^{-4}$ | −1.55 |
| −17.10 | 2182/9/24.93 | −0.92 | $3.20 \times 10^3$ | $2.76 \times 10^{-4}$ | −1.52 |
| −15.43 | 2185/9/24.60 | −0.59 | $5.45 \times 10^4$ | $2.60 \times 10^{-5}$ | −2.56 |
| −15.02 | 2189/9/24.62 | −0.50 | $8.07 \times 10^4$ | $1.60 \times 10^{-5}$ | −2.78 |
| −20.44 | 2192/9/24.35 | −1.59 | $1.08 \times 10^4$ | $4.40 \times 10^{-5}$ | −2.34 |
| −16.27 | 2195/9/24.34 | −0.75 | $6.33 \times 10^4$ | $2.00 \times 10^{-5}$ | −2.70 |
| −7.51 | 2199/9/25.05 | +1.00 | $1.89 \times 10^4$ | $5.40 \times 10^{-5}$ | −2.27 |

As reflected in Table 2 and Fig. 4, there are many more VIs for different years, but the year 2182 dominates the overall IP, so much that we wish to identify the apparently special dynamical behavior that would cause such a large region in the initial conditions space to impact.

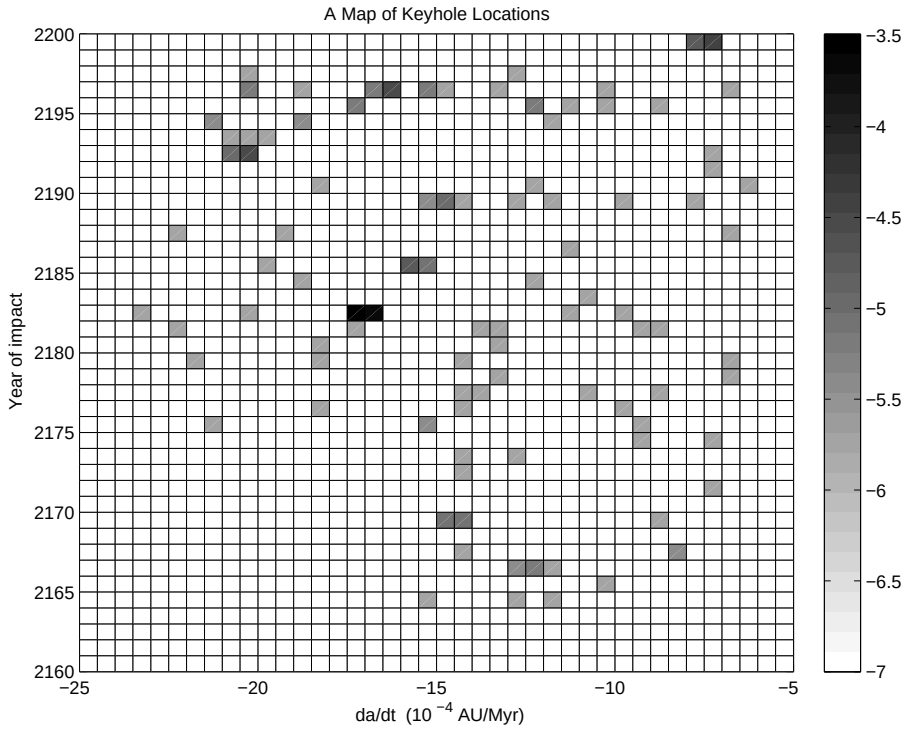


Figure 4: The distribution of the impactors found in the MC run as a function of the secular drift in semimajor axis due to Yarkovsky and the impact year. The shading is according to $\log_{10}$ of the probability of impact obtained for each cell.

# 5 Line of Variations Impact Monitoring

The standard method used for impact monitoring is the *Line Of Variation* (LOV) search [Milani et al. 2005b], based on the computation of multiple initial orbits sampling the LOV, which is essentially a line of weakness in the initial conditions space. The LOV definition depends upon the choice of coordinates [Milani et al. 2005a]; in this case we have used Keplerian elements and a scaling such that the LOV is essentially along the $a$ axis, as it is appropriate when the time span is so long that the along track runoff is the dominant uncertainty.

We have used the CLOMON2 version of the impact monitoring algorithm, in use at the Universities of Pisa and Valladolid, which is also available in the free software *OrbFit*; the SENTRY version, in use at JPL, is based on similar principles, although implemented differently [Milani et al. 2005b]. These software robots have been developed to monitor possible impacts in the medium term, say 10 to 100 years from now, and thus do not currently have the capability of fully taking into account Yarkovsky and other non-gravitational perturbations. For example, we cannot yet sample a LOV in 7-dimensional space and use it to find VIs in that space. We can include different forms of Yarkovsky effect in the dynamical model, including the assumption of an acceleration in the transversal direction, with an $1/r^2$ dependence upon the heliocentric distance $r$, which results in a secular $da/dt$. The constant value of $da/dt$ can be set for each run, thus we can explore a 6-dimensional section in the 7-dimensional space of the MC runs.

We have performed 7 runs of CLOMON2, involving 2401 VAs each, with values of $da/dt$ ranging from $-17.4$ to $-16.8$ with step 0.1 in units of $10^{-4}$ AU/My. This samples the range of $da/dt$ where most of the MC impacts in 2182 are: Figure 5 shows the MC sample orbits with impact in 2182 and the LOV sample orbits with impact in 2182. The latter are joined by segments whenever they belong to consecutive sample points on the LOV to stress that our impact monitoring uses geometric sampling, a version of *manifold dynamics*, in which we can interpolate smoothly between sample points.

The CLOMON2 algorithm can indeed interpolate and find, for each of the 14 segments, the point corresponding to the closest approach to the center of the Earth and compute the estimated IP: the values obtained in this way for 2182 the impacts range between $1.6 \times 10^{-3}$ and $2.1 \times 10^{-2}$. These are not correct estimates of the impact probability under the present level of information about the orbit, because they are conditional probabilities for a given, fixed value of $da/dt$; still these values give an indication of what could happen if the value of $da/dt$ was well known.

The most striking feature of Fig. 5 is the presence of two VIs, that is two separate components, each connected, in the region of initial conditions (in the 7-dimensional space) leading to an impact in 2182. This could be figured out by using the MC points, but is demonstrated rigorously by using the LOV sampling. The VAs consecutive as LOV sample points leading to a 2182 impact are connected by a line segment; however, between the segments on the left of the figure and the ones on the right, there are Virtual Asteroids on each LOV not leading to an impact.

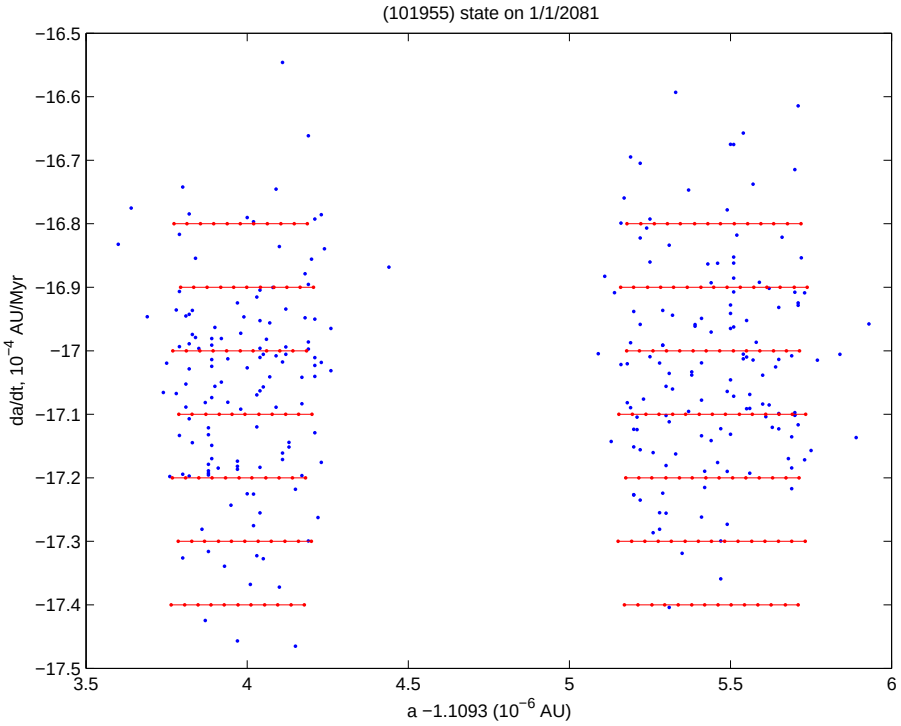


Figure 5: The Virtual Asteroids impacting in 2182, in the same plane as Fig. 3, with $da/dt$ and semimajor axis at epoch January 1, 2081, that is after the 2080 close approach. The MC impactors are represented as isolated points, the consecutive LOV sample orbits which impact are represented as connected strings.

The explanation can be found by looking at the 2182 *Target Plane*[3] (TP) trace of the MC and LOV computations. In Fig. 6 we show the MC points on the 2182 TP, including the impactors and also the near-miss points. Note that, although the MC points have been selected at random, according to a probability density, in the 7-dimensional space, still most of the impactors and near-miss points are organized in a very narrow strip entering the figure from the top, crossing the Earth impact cross section, and leaving the latter from the bottom. The strip then reverses, crossing again the impact cross section and reaching back to the upper boundary of the plot window. A similar figure done with the 7 LOV sampling runs shows 7 strings doing the

[3]Hereafter we use TP coordinates defined as in [Valsecchi et al. 2003].

same as the MC strip: they are so tightly packed that the human eye would not be able to separate them at the scale of the plot.

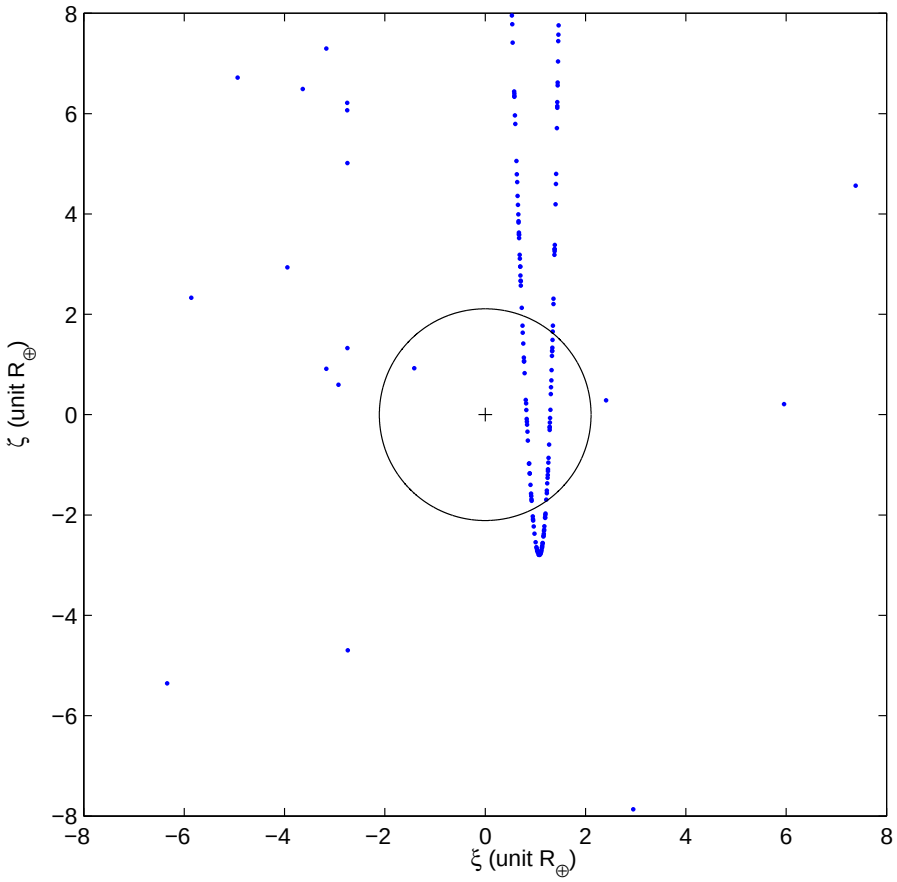


Figure 6: The Target Plane traces of the MC sample orbits which have a very close approach in 2182; the coordinates are as in [Valsecchi et al. 2003], units are Earth radii.

The key point is that the very same reason why there are two separate VIs is also the cause of the especially high IP associated to the two VIs. Indeed, if the LOV strings "stop and come back", this implies that the derivative $d\zeta/d\sigma$ of the vertical coordinate in the Figure with respect to the LOV parameter $\sigma$ has a zero [4], then changes sign. This is called an *interrupted return*

[4]Note that the $\sigma$ used here to parameterize the LOV is from CLOMON2 runs for fixed $da/dt$, and thus is not the same as that of Table 2.

[Milani et al. 1999, Milani et al. 2005b, Valsecchi et al. 2003]. Since $d\zeta/d\sigma$ is a smooth function, it has smaller values near the tip. This also affects the *stretching* $S$, which is the length of the derivative of the TP point with respect to the LOV parameter $\sigma$. In most points (except near the tip) the contribution of $|d\zeta/d\sigma|$ in $S$ is dominant. However, $S$ is sharply reduced near the tip, thus the TP points near the tip are closer to each other. Because the tip where the strings turn back is very close to the segments contained in the Earth cross section, more sample points belong to the two VIs.

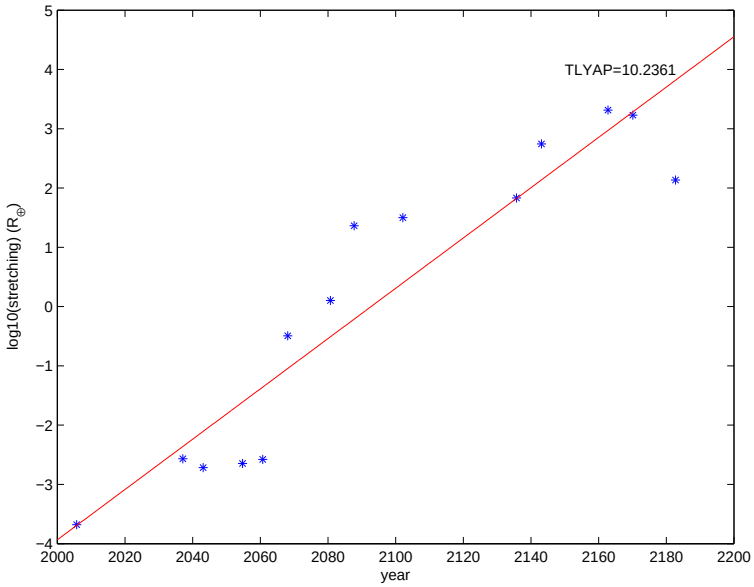


Figure 7: The stretching (in a $\log_{10}$ scale) generally increases at each close approach with Earth, but not at all of them. These data refer to the sample orbit of 1999 $RQ_{36}$ nearest to the center of the VI on the left in Fig. 5. The stretching on average grows by an order of magnitude in 23.6 years, thus by a factor exp(1) on average every 10.2 years.

To assess the importance of this phenomenon, we have plotted in Fig. 7 the behavior of $S$ at successive close approaches with Earth. The stretching generally increases, by a factor exp(1) on average every 10.2 yr (this could be used as an estimate of the so called *Lyapounov time*). The Figure in fact shows that the stretching increases by about 1 order of magnitude until 2060, then the close approaches in 2060, 2068 and 2080 increase it by 4 orders of magnitude, followed by moderate growth until 2170. After the close approach

of 2170 there is a decrease by a factor $\simeq 16$, which is one way of explaining why the two largest VIs for 2182 have an IP an order of magnitude larger than all of the others found in the MC run.

# 6 Interpretation

To explain the very complex dynamics leading to especially large VIs, we shall partition the time span from the initial conditions time in 2001 to the impact in 2182 in 4 phases, using the previous Figures, Table 3 with the close approaches for one of the 268 VAs with similar close approach sequence impacting 2182 and the following order of magnitude argument: a Yarkovsky perturbation of the order of $10^{-3}$ AU/My corresponds to 15 km/100 yr. The discussion hereafter concerns the region of the LOV encompassing the 2182 VIs.

Table 3: Close Approach Summary for a VA impacting in 2182.

| Date | CA Dist AU | Vinf km/s | Stretch. $R_\oplus$ |
|---|---|---|---|
| 2005 Sep 20.45 | 0.0331 | 6.8 | $2.30 \times 10^{-4}$ |
| 2037 Feb 11.56 | 0.0987 | 7.5 | $3.79 \times 10^{-3}$ |
| 2043 Feb 09.76 | 0.0966 | 4.3 | $1.66 \times 10^{-3}$ |
| 2054 Sep 30.04 | 0.0393 | 5.1 | $1.62 \times 10^{-3}$ |
| 2060 Sep 23.03 | 0.0050 | 6.1 | $2.71 \times 10^{-3}$ |
| 2068 Feb 15.14 | 0.0705 | 5.7 | $3.16 \times 10^{-1}$ |
| 2080 Sep 22.09 | 0.0149 | 6.3 | $1.38 \times 10^{+0}$ |
| 2087 Sep 29.83 | 0.0418 | 5.0 | $1.69 \times 10^{+1}$ |
| 2102 Feb 17.22 | 0.0779 | 4.9 | $2.38 \times 10^{+1}$ |
| 2135 Sep 27.82 | 0.0222 | 5.5 | $5.79 \times 10^{+1}$ |
| 2143 Feb 16.44 | 0.0776 | 5.0 | $4.41 \times 10^{+2}$ |
| 2162 Oct 19.05 | 0.0936 | 4.4 | $1.14 \times 10^{+3}$ |
| 2170 Feb 17.69 | 0.0927 | 7.5 | $2.63 \times 10^{+3}$ |

In phase 1 (2001–2060), the change in $a$ due to Yarkovsky is much larger than the conditional uncertainty (for fixed $da/dt$) of the semimajor axis: $RMS(a) \simeq 5$ m. Thus the solutions with different values of $da/dt$ are well

separated. Upon arrival on the Target Plane of the 2060 encounter, the traces on the TP of the 7 VIs of our 7 CLOMON2 runs are still well separated, by $\simeq 80$ km, while the segments of the LOV leading to the 2182 impact are only a few hundred meters long.

In phase 2 (2060–2080), a sequence of 3 close approaches, in 2060 near the ascending node, in 2068 near the descending node, and in 2080 near the ascending node again, increases the stretching (as measured at the next encounter in 2087) by a factor $\simeq 9,000$.

In phase 3 (2080–2162), the orbits compatible with the current observational data are scattered widely and follow different dynamical routes. The spread in semimajor axis after the 2080 encounter can be seen in Fig. 3, top, for the whole set of VAs used in the MC run, and is $\simeq 600,000$ km. For the subset leading to the main 2182 VIs, as shown in Fig. 5, the range of values in $a$ is $\simeq 90$ km wide for the larger VI (on the right) and $\simeq 60$ km for the one on the left. Thus the total effect of Yarkovsky on the semimajor axis in the time span 2081–2182 is less than the span in $a$ of the VIs, and quite negligible with respect to the spread in 2081. From there on, it is the value of the semimajor axis that determines which dynamical route will be followed, that is the sequence of close approaches to the Earth, while the value of $da/dt$ will not have much influence, as it can only displace slightly the position of the keyhole on exit from the 2080 encounter.

Phase 4 (2162–2182) begins with the shallow (for the LOV portion we are discussing) approach near the ascending node in 2162, and leads to the deep encounter near the ascending node in 2182 with a reduced stretching and two separate VIs. This phase has to be investigated by using the theory of *resonant returns* [Milani et al. 1999], [Valsecchi et al. 2003], [Milani et al. 2005b], see below.

The sequence of phases 1, 2 and 3 is not that unusual. For (99942) Apophis, phase 1 —in which the Yarkovsky effect is the dominant source of uncertainty [Chesley 2006, Giorgini et al. 2008] — lasts until the 2029 very close approach to the Earth. Phase 2 contains only the 2029 encounter, which increases the spread in $a$, resulting in an increase of the stretching at the next encounter by a factor $\simeq 40,000$. In phase 3, leading to a possible impact in 2036, the effect of Yarkovsky and other nongravitational perturbations is not important in determining the outcome.

Phase 4 in the evolution of our 2182 VIs is a manifestation of an *interrupted resonant return*. As shown in Fig. 6, the line of VAs arriving on the 2182 target plane has a fold, with the tip near the Earth impact

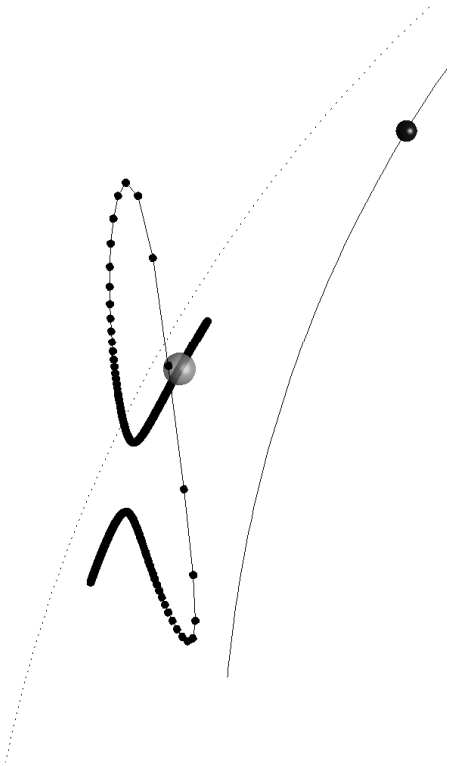

Figure 8: The position, projected on the ecliptic plane, of the VAs forming a segment of the LOV 5 months after the September 2162 close approach to the Earth (the dark sphere, not to scale). The transparent sphere marks the segment of the LOV where the impactors in 2182 are located. The spacing between consecutive VAs corresponds to $\Delta\sigma = 0.0025$.

cross section. In the cases of interrupted resonant returns described so far [Milani et al. 2000b] the fold occurs before the Earth is reached while, in 2182, 1999 $RQ_{36}$ can have what we may call a *failed interrupted resonant return*: the line of VAs turns back on the TP too late, beyond the Earth cross section.

This fold —or, better, the entire Ω-shaped set of four folds shown in Fig. 8— was generated in 2162. For example, if we use the CLOMON2 run with $da/dt = -17.1 \times 10^{-4}$ AU/My, the closest approach in 2162, at 14.2 Earth radii, occurs for a value of the LOV parameter[5] $\sigma = +0.868$, while

[5]Note that the $\sigma$ used here to parameterize the LOV is from CLOMON2 runs for fixed

the two 2182 VIs are centered at $\sigma = -0.267$ and $\sigma = -0.361$. However, one of the folds generated by the 2162 close approach travels along the LOV towards negative values of $\sigma$: in 2170 it has reached $\sigma = 0.2$, and by the time of the 2182 close approach the fold is at $\sigma = -0.311$, right in between the two VIs.

Figure 8 shows the $\Omega$-shaped perturbation introduced in the LOV by the 2162 close approach to the Earth. As expected from the analytic theory [Valsecchi et al. 2003], [Milani et al. 2005b, Section 3.2], a planet passing near the sequence of VAs introduces four folds and opens a gap. The two folds corresponding to the stronger perturbations have the special property that the decrease in stretching is roughly compensated by increase in width [Milani et al. 2005b, Appendix B], while the two corresponding to weaker perturbations result in a smaller increase in stretching without a corresponding decrease of width.

In 2163, the larger VIs of 2182 are *near* one of the folds of the latter kind, but not *at* the fold, as shown in Fig. 8. The fold moves along the LOV like a wave because there is a gradient of semimajor axis —along the LOV segment that we are considering— that has the same sign as the gradient of the mean anomaly. Consequently, as time passes, the leading VAs, which are characterized by a smaller mean motion, start to lag, so that the $\sigma$-coordinate of the fold changes, and the fold point rolls along the LOV. In 2182 it has moved so much that it happens to be just between the two strings of consecutive VIs shown in Figs. 5 and 6. The close packing of VAs near the tip of the fold reflects the drop of the stretching $S$ in phase 4, as shown in Fig. 7.

# 7 What happens next?

Given a possibility of impact so remote in the future, the question arises whether there can be changes in the situation in the short term. 1999 $RQ_{36}$ is currently behind the Sun and cannot be observed until the spring of 2011. In that year it will undergo a close approach to Earth with a minimum distance 0.177 AU on September 11, 2011.

The most favorable time for optical observations will be around August 30, with a formal prediction uncertainty of 0.02 arcsec (longest axis of $\sigma = 1$

$da/dt$, and thus is not the same as that of Table 2; the values we mention are from the run with $da/dt = -17.1 \times 10^{-4}$ AU/Myr.

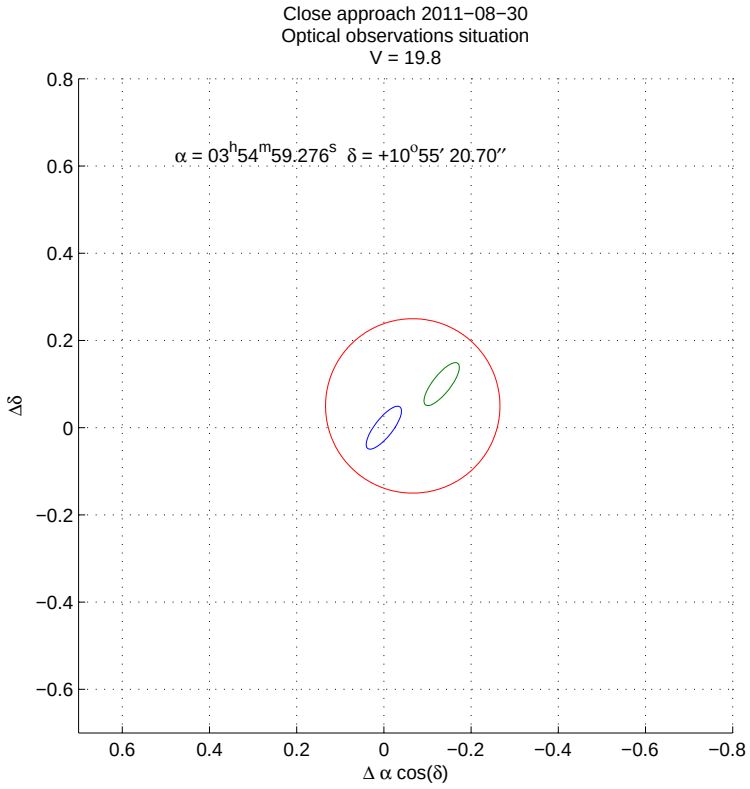


Figure 9: Celestial sphere coordinates (right ascension and declination, in arcsec) relative to the nominal prediction without Yarkovsky for the recovery of 1999 $RQ_{36}$ on August 30.0, 2011. The confidence ellipses are drawn for both cases: no-Yarkovsky (on the left) and $da/dt = -17.1 \times 10^{-4}$ AU/My (on the right). The circle has a radius of 0.2 arcsec.

confidence ellipse). Figure 9 shows the confidence ellipse computed from an orbital solution with no Yarkovsky effect (on the left) and the one computed from an orbital solution with a value of the secular $da/dt = -17.1 \times 10^{-4}$ AU/My (on the right). The two confidence ellipses, drawn for a $3\sigma$ confidence level, are indeed disjoint, which means that there is a significant signal to discriminate between the two cases. The problem is that the noise contained in the 2011 optical observations is likely to confuse the results. We have drawn in the figures a circle with a radius of 0.2 arcsec, which is larger than the difference in the predictions due to the Yarkovsky effect to be measured. Note that by taking many accurate observations it would certainly be

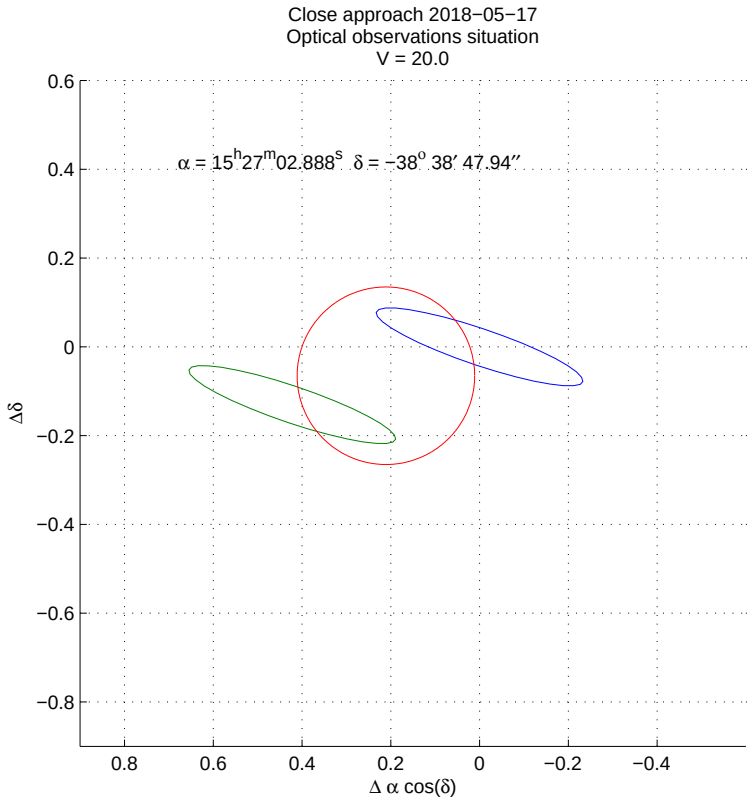


Figure 10: Prediction for recovery of 1999 $RQ_{36}$ on May 17.0, 2018, plotted with confidence ellipses as in the previous figure: the no-Yarkovsky case (on the right) and $da/dt = -17.1 \times 10^{-4}$ AU/My (on the left). The circle has a radius of 0.2 arcsec.

possible to average out the random astrometric errors at a level lower than the Yarkovsky signal, but this would not at all solve the problem, because systematic errors in the astrometric data would not be removed.

In fact, as pointed out by [Carpino et al. 2003], strong correlations and biases in the astrometric errors, presumably due mostly to catalog regional errors [Tholen et al. 2008, da Silva Neto et al. 2005], at present do not allow absolute astrometry better than about 0.2 arcsec. It is possible that by 2011 this problem will be solved with the production of a statistically sound astrometric error model, removing the main biases and accounting correctly for the correlations; work to this goal is currently under way [Baer et al. 2008].

In May 2018 there are again favorable conditions to observe 1999 $RQ_{36}$ and to obtain optical astrometry. As shown in Fig. 10, at that time the signal caused by the Yarkovsky effect would be marginally significant with respect to the level of error corresponding to the current state of the art. However, by that time it can be presumed that the quality control of optical astrometry would have progressed, both because of a better statistical quality control on the past observations and because of the results of the next generation surveys, such as Pan-STARRS and LSST. In 2024 the situation would be even better, with a Yarkovsky signal of the order of 1 arcsec which should provide a tight constraint on the value of $da/dt$.

To acquire information on the Yarkovsky effect acting on 1999 $RQ_{36}$ in a shorter time frame the best opportunity is to use radar astrometry during a comparatively close approach in 2011. With a distance exceeding 26 million km this requires a very powerful radar system, but the declination at the time of closest approach is $+20°$, thus the observing conditions are favorable for the Arecibo radar, which has observed (99942) Apophis at a larger distance. We have assumed that the measurement error would be similar to the one of the Arecibo observations of Apophis in January 2005, that is RMS in range of 0.6 km and in range-rate of 1 km/d, and simulated[6] two range and two range-rate observations on 29-31 August 2011. With these prospective measurements, we have repeated the procedure of Section 3 and obtained an estimated $da/dt$ uncertainty of $\pm 0.25 \times 10^{-4}$ AU/Myr. Thus the 2011 observations from Arecibo should reduce the RMS uncertainty by a factor $\simeq 40$ with respect to the analogous result with the present data, and by a factor $\simeq 20$ with respect to the a priori uncertainty in the model of Eq. (1).

Of course, the most likely outcome would be a contradiction between the radar data and the large 2182 VIs. However, judging from Fig. 3, it is very likely there would be other VIs which would be confirmed and could increase their estimated IP. For any VIs that remain near nominal, the increase of the probability density due to the decreased uncertainty could result in an increase of the IP by a factor $\simeq 15$. Anyway there would be a very significant increase in the level of information on this orbit, resulting in changes to the VIs and their IPs.

There is another way to improve the knowledge of the nongravitational

[6]We have used in the simulation observations from the Arecibo planetary radar. The distance of 1999 $RQ_{36}$ during the 2011 close approach and the size of the object would make an observation from Goldstone difficult.

perturbations acting on 1999 $RQ_{36}$: by close-up observations from a spacecraft it is possible to determine accurately the parameters of Table 1. With an orbiter it would be possible both to develop a full nongravitational perturbations model, by using visible and infrared images, and to measure the corresponding perturbations with a radioscience experiment. 1999 $RQ_{36}$ was the target of the mission OSIRIS proposed to NASA, and is among the possible targets of the Marco Polo mission proposed to ESA.[7] Improving the fidelity of asteroid thermal measurements and models, which will allow, among other applications, the development of more accurate models for the Yarkovsky effect, should be included among the main scientific goals of the next generation of asteroid missions.

# 8 The deflection problem

To complete the worst case analysis, we need to discuss how difficult it would be to deflect 1999 $RQ_{36}$ from a collision course in case it was confirmed by very accurate observations in the next decades. The answer is implicitly contained in Fig. 7: a deflection maneuver performed before "phase 2", the sequence of close approaches of 2060–2080, is comparatively easy, after 2080 the challenge increases dramatically.

On the target plane of the 2060 encounter the *keyhole* [Valsecchi et al. 2003, Chodas 1999], that is the pre-image of the Earth in the 2182 TP, for a fixed value of $da/dt$ and for a given VI, is a thin crescent with width less than a km. The TP trace of the VI is the intersection of the TP confidence region with this crescent: a deflection can be obtained by achieving a displacement in 2060 by an amount of this order.

Thus, if the deflection maneuver was performed after the Yarkovsky effect has been well constrained but before the beginning of phase 2, that is before 2060, the required change in velocity of the asteroid would be very small, to the point that it would not be a problem even by the technology available today, e.g., with the kinetic deflection method[8].

Immediately after the 2080 encounter, the amount of velocity change needed to deflect away from the 2182 impact would be much larger: as

[7] Neither of the two missions is presently fully approved and funded.

[8] For a description of this method, see the ESA study Don Quijote [Milani and Gronchi 2009, Chap. 14].

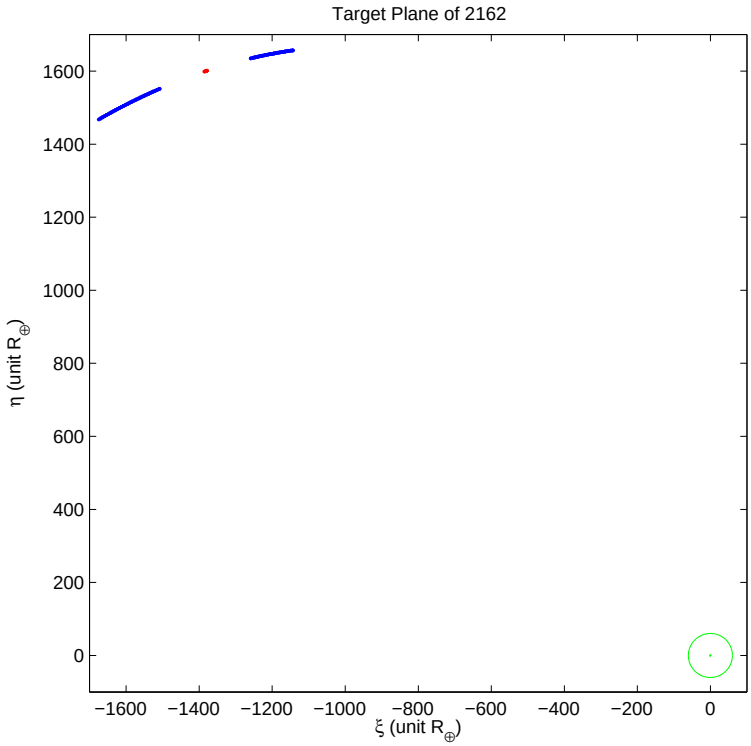


Figure 11: The double keyhole for the impact in 2182 as seen on the target plane of the 2162 encounter. We have plotted also the points corresponding to the fold, that is corresponding to the lower tip just below the Earth impact cross section in Fig. 6. For comparison, we have plotted a circle around the Earth with radius equal to the mean radius of the Moon's orbit.

shown in Figure 5, a change in semimajor axis to deflect out of each of the two largest VIs would be of the order of several tens of km.

In phase 3 the stretching increases slowly, and so does the required velocity change, with a peak value in 2162. On the target plane of the 2162 encounter, the two VI traces of 2182 appear as two very long stretches with length $\simeq 187$ and $\simeq 118$ Earth radii, respectively, as shown in Fig. 11. Because of the *failed interrupted resonant return*, the stretching between 2162 and 2182 actually decreases, thus "the keyhole is larger than the door", that is the TP points leading to the impact form a figure with a width comparable to the diameter of the Earth impact cross session and a much larger length. To deflect with a maneuver shortly before 2162 would need an off-track im-

pulse, changing the 2162 TP trace by a significant fraction of $R_\oplus$.

The current impact monitoring covers a time span of about a century. If this were to continue, and the asteroid 1999 $RQ_{36}$ were indeed on a collision course for 2182, then the warning about this would be issued only in 2082, that is at a time when the opportunity to deflect with requirements compatible with current technology would already be expired. To extend the predictability horizon of impact monitoring seems to us to be a better solution, at least economically, than waiting for future and hypothetical technological advances.

# 9 Conclusions and Future Work

The analysis presented in this paper represents a step toward the extension of the predictability horizon for Earth impacts of NEAs to a time scale of several centuries. The main reason for trying to push this horizon further away in time is that, in case a deflection is needed for an Earth impactor, the available time is a non-renewable "scarce resource". The example we have analysed shows that the cost of deflection, although it is generally growing when waiting before the action, may remain at very high levels for extended periods of time before the impact date.

Of course, longer time spans imply more room for the NEA to display the chaoticity of its motion, especially in cases, like the one discussed here, of rather frequent planetary encounters. Concerning the understanding of encounter-dominated, strongly chaotic orbits, the analytical theory developed so far [Valsecchi et al. 2003, Milani et al. 2005b] has been strongly confirmed, but it does not yet address the issue of how folds, once developed at an encounter, propagate along the LOV. This aspect is now the object of ongoing research by our team.

The dynamics over longer times of moderate size asteroids is also affected by nongravitational forces. As a consequence, the effort must pursue significant improvements of the modeling of the various nongravitational forces that can affect NEAs on multi-century time scales. Such progress depends also upon theoretical studies, but mostly upon the availability of stringent observational constraints, which can be provided by increased accuracy optical astrometry (with reliable error models), radar astrometry, physical characterization observations from the ground and from space, including in situ missions.

The results on the specific case of the asteroid 1999 $RQ_{36}$ have been obtained with a dedicated effort, and at the moment we do not have the capability to extend a comparable scan for impacts over a longer time span and over a wider range of perturbation parameters to all the objects with good enough orbits. Whether the results obtained for 1999 $RQ_{36}$ are typical rather than exceptional we do not know yet.

However, we already know another example of a numbered NEA for which impact monitoring can be extended beyond the 100 years horizon: (153814) 2001 $WN_5$. In comparison with 1999 $RQ_{36}$ this is a somewhat larger asteroid[9], with no radar observations and therefore a less well determined orbit: RMS($a$) $\simeq$ 15 km. In 2028 this asteroid has a deep encounter (minimum distance $\simeq 40\ R_\oplus$), resulting in a sharp increase of the stretching, which we can describe as the beginning of phase 2.

The main difference with the main case discussed in this paper is that for 2001 $WN_5$ the Yarkovsky effect does not matter in the impact monitoring, even for an extended time span, because the effect of the possible values of $da/dt$ over the timespan of phase 1, that is until 2028, is much smaller than RMS($a$). Given the possible size of this object, a plausible range of secular semimajor axis drift due to Yarkovsky could be in the range $|da/dt| < 12 \times 10^{-4}$ AU/My; the sign is not known because we have no information on the spin axis. This translates in changes of $a$ in 20 years up to 3.6 km, corresponding to about 1/4 of RMS($a$): the large relative uncertainty on the Yarkovsky effect is not the main contributor in the uncertainty budget for the 2028 TP trace. Thus the trace of the confidence region on the 2028 TP is only slightly larger when considering the uncertainty in $da/dt$ with respect to the one from a purely gravitational model.

This implies that it is possible to use the currently operational impact monitoring systems CLOMON2 and SENTRY, just extending the time horizon, to find VIs and estimate the corresponding IP. The result has been to find a comparatively large VI for the year 2133, with an estimated IP of $10^{-5}$. Figure 12 shows the behavior of the stretching $S$, showing clearly a phase 1 with modest growth of $S$ until 2028, a phase 2 containing the 2028 encounter only (very much like Apophis), followed again by a moderate growth of $S$ in phase 3. The value of the IP for the 2133 VI is not as big as that for 1999 $RQ_{36}$ in 2182 because there is no phase 4, that is no interrupted return. Still,

[9] 2001 $WN_5$ has absolute magnitude $H = 18.2$ instead of 20.8 for 1999 $RQ_{36}$. However, the size is very poorly constrained because the taxonomic type is still unknown.

this could become a critical case for deflection if the VI of 2133 were confirmed by post-2028 observations, because the amount of required deflection would already be large.

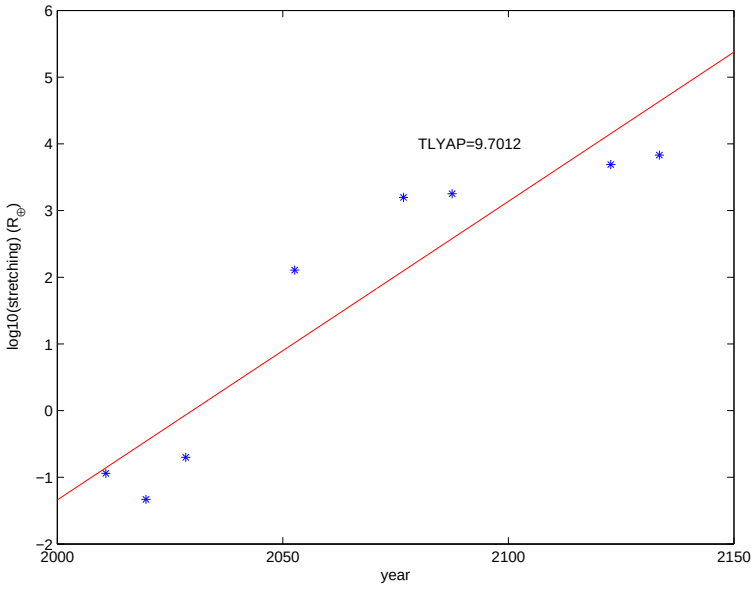


Figure 12: The stretching (in a $\log_{10}$ scale) at each close approach with Earth for the sample orbit of 2001 $WN_5$ nearest to the center of the 2133 VI. The stretching on average grows by a factor exp(1) on average every 9.7 years.

The conclusion we can draw is that the set of NEAs with low MOID and well determined orbits could contain a significant number of cases for which an extended impact monitoring would give interesting results, but we should not expect that these additional cases would have the same properties of the ones already found.

Another implication is that impact monitoring needs to be continued forever: even when an asteroid has an extremely well determined orbit, at some future time it could undergo a "phase 2" with one or more very close approaches, increasing the stretching to the point that collision solutions become possible later, and would become easily detectable from the orbit solution with observations during "phase 3". This is already known, for a very far future, for (4179) Toutatis [Ostro et al. 1999] and (29075) 1950 DA [Giorgini et al. 2002].

To be ready to extend the predictability horizon for impact monitoring,

and to handle the unknown parameters contained in the nongravitational perturbations, we need to set up our algorithms for full orbit determination in a space of dimension at least 7 (including either $da/dt$ or similar empirical parameters), for the computation of the LOV in such space, and for minimization of the close approach distance in this context. Moreover, the numerical accuracy requirements are severe and need to be carefully addressed for reliable semiautomatic operations.

# Acknowledgments

We wish to dedicate this paper to the memory of Steve Ostro (1946-2008), who pioneered the radar observations of asteroids, so essential for these studies.

We thank Mike Nolan and collaborators for making available their preliminary analysis of the spin axis orientation of 1999 $RQ_{36}$, and Carl Hergenrother for providing a precise estimate of the spin rate of the asteroid.

The authors have been supported by: the Italian Space Agency, under contract ASI/INAF I/015/07/0, Tasks 3130 and 3430 (A.M., G.B.V. and F.B.); the Spanish *Ministerio de Ciencia y Tecnología* through the grant AYA2007-64592 and by the *Junta de Castilla y León* through the grant VA060A07 (M.E.S. and O.A.). The work of S.R.C. was conducted at the Jet Propulsion Laboratory, California Institute of Technology, under a contract with the National Aeronautics and Space Administration.

# References

[Baer et al. 2008] Baer, J., Milani, A., Chesley, S.R. and Matson, R.D., 2008. An Observational Error Model, and Application to Asteroid Mass Determination, AAS-DPS meeting 2008, abstract 52.09.

[Carpino et al. 2003] Carpino, M., Milani, A., Chesley, S.R., 2003. Error Statistics of Asteroid Optical Astrometric Observations. Icarus 166, 248–270.

[Chesley 2006] Chesley, S.R., 2006. Potential impact detection for Near-Earth asteroids: the case of 99942 Apophis (2004 $MN_4$), ACM2005 IAU-229, 215–228.

[Chesley 2008] Chesley, S.R., abstract ACM 2008.

[Chodas 1999] Chodas, P.W. 1999. Orbit uncertainties, keyholes, and collision probabilities, BAAS 31-1117.

[Chodas and Yeomans 1999] Chodas, P.W. and Yeomans, D.K. 1999. Predicting close approaches and estimating impact probabilities for near-Earth objects. Paper AAS 99-462, AAS/AIAA Astrodynamics Specialists Conference, Girdwood, Alaska.

[Giorgini et al. 2002] Giorgini, J.D., Ostro, S.J., Benner, L. A.M., Chodas, P.W., Chesley, S.R., Hudson, R.S., Nolan, M.C., Klemola, A.R., Standish, E.M., Jurgens, R.F., Rose, R., Chamberlin, A.B., Yeomans, D.K. and Margot, J.-L. 2002. Asteroid 1950 DA's Encounter with Earth in 2880: Physical Limits of Collision Probability Prediction. Science 296, 132–136.

[Giorgini et al. 2008] Giorgini, J.D., Benner, L. A. M., Ostro, S. J., Nolan, M. C. and Busch, M. W., 2008. Predicting the Earth encounters of (99942) Apophis, *Icarus* **193**, 1–19.

[Gronchi 2005] Gronchi, G. F., 2005. An algebraic method to compute the critical points of the distance function between two Keplerian orbits, *CMDA* **93**, 297–332.

[Gronchi and Tommei 2006] Gronchi, G. F. and Tommei, G. 2006. On the uncertainty of the minimal distance between two confocal Keplerian orbits, *DCDS-B* **7/4**, 755–778.

[Milani and Gronchi 2009] Milani, A. and Gronchi, G.F. 2009. *The Theory of Orbit Determination*, Cambridge University Press, in press.

[Milani et al. 1999] Milani, A., Chesley, S.R., and Valsecchi, G.B. 1999. Close approaches of asteroid 1999 $AN_{10}$: Resonant and non-resonant returns. Astron. Astrophys. 346, L65–L68.

[Milani et al. 2000a] Milani, A., Chesley, S.R., Boattini, A., and Valsecchi, G.B. 2000. Virtual impactors: Search and destroy. *Icarus* 145, 12–24.

[Milani et al. 2000b] Milani, A., Chesley, S.R., and Valsecchi, G.B. 2000. Asteroid Close Encounters with Earth: Risk Assessment. *Planetary and Space Science* 48, 945-954.

[Milani et al. 2005a] Milani, A., Sansaturio, M.E., Tommei, G., Arratia, O., Chesley, S.R., 2005. Multiple solutions for asteroid orbits: computational procedure and applications. Astron. Astrophys 431, 729–746.

[Milani et al. 2005b] Milani, A., Chesley, S.R., Sansaturio, M.E., Tommei, G., Valsecchi, G., 2005. Nonlinear impact monitoring: Line Of Variation searches for impactors. Icarus 173, 362–384.

[Morrison 1992] Morrison, D., ed., 1992. The Spaceguard survey: report of the NASA International Near-Earth-Object Detection Workshop, Pasadena, CA. Jet Propulsion Laboratory/California Institute of Technology, 1992.

[Nolan et al. 2007] Nolan, M. C., Magri, C., Ostro, S. J., Benner, L. A. M., Giorgini, J. D., Howell, E. S., Hudson, R. S., 2007. The Shape and Spin of 101955 (1999 RQ36) from Arecibo and Goldstone Radar Imaging. AAS-DPS meeting 2007, abstract 13.06.

[Ostro et al. 1999] Ostro, Steven J., Hudson, R. Scott, Rosema, Keith D., Giorgini, Jon D., Jurgens, Raymond F., Yeomans, Donald K., Chodas, Paul W., Winkler, Ron, Rose, Randy, Choate, Dennis, Cormier, Reginald A., Kelley, Dan, Littlefair, Ron, Benner, Lance A. M., Thomas, Michael L. and Slade, Martin A., 1999. Asteroid 4179 Toutatis: 1996 Radar Observations. *Icarus*, 137, 122–139.

[da Silva Neto et al. 2005] da Silva Neto, D. N., Andrei A. H., Assafin, M., Vieira Martins, R., 2005. Investigation on the southern part of the high density astrometric catalogs USNO B1.0, 2MASS and UCAC2. Astron. Astrophys 429, 739–746.

[Tholen et al. 2008] Tholen, D.J., Bernardi, F., and Micheli, M. 2008, Where is Apophis?, AAS/Division for Planetary Sciences Meeting Abstracts, 40, #27.02

[Valsecchi et al. 2003] Valsecchi, G.B.,Milani, A., Gronchi, G.-F., Chesley, S.R., 2003. Resonant returns to close approaches: analytical theory. Astron. Astrophys 408, 1179–1196.

[Vokrouhlický et al. 2000] Vokrouhlický, D., Milani A. and Chesley, S.R. 2000. Yarkovsky effect on small Near Earth asteroids: mathematical formulation and examples. Icarus 148, 118–138.